

Feasible Development of a Carbon-Based MEMS Using a MEMS Fabrication Process

Junji Sone*

Faculty of Engineering, Tokyo Polytechnic University, Atsugi 243-0297, Japan

Abstract: We aimed to develop a process technology for constructing a carbon-based micro-electromechanical system that does not require a high-temperature and high-energy process. A HOPG (highly oriented pyrolytic graphite) crystal microsheet was prepared by exfoliation. Cantilevers and doubly clamped beams were patterned using a photoresist. The HOPG microsheet was attached by using a tantalum layer. We fabricated cantilevers and a doubly clamped beam by controlling the thickness of the HOPG microsheet and then measured the first resonance frequency. The measurements suggest a need to improve the stiffness of the beam.

Key words: Carbon-MEMS (micro-electromechanical systems), cantilever, trial fabrication, resonance frequency, Raman spectra, HOPG.

1. Introduction

Carbon nanotubes, fullerenes and graphene are materials that are useful in the fabrication of electrical devices (e.g., transistors, electrical wires and batteries), MEMS (micro-electromechanical systems) [1], and nanomechanical technologies [2]. These materials have high mechanical strength, high electrical mobility, chemical stability and high thermal conductivity. The primary goal of our research, therefore, was to develop a MEMS device that exhibits superior mechanical properties. Many studies have been done on HOPG (highly oriented pyrolytic graphite) crystal using graphene that can undergo multiple exfoliations.

A freestanding, high-carbon structure for MEMS devices [3, 4] was fabricated by using glassy carbon. Molding and soft lithography were performed to obtain structures with a smooth shape. The carbon used was pyrolyzed from polymeric precursors. The carbon-based materials exhibited a porous microstructure, shrinkage deformation and pyrolysis temperature that was slightly higher than that required

for a MEMS device. Rose et al. [5] fabricated a cantilever through direct mechanical cleavage of a bulk HOPG crystal on silicon micropillars by using a focused ion beam, which requires micropillars. They fabricated these structures using a focused ion beam, which requires micropillars. Chen et al. [6] also fabricated monolayer doubly clamped beams by using monolayer graphene flakes. A resonance frequency was observed to be near 65 MHz. Cantilevers and doubly clamped beams with thicknesses varying from a single atomic layer to 75 nm were fabricated. Bunch et al. [7] observed resonance frequencies varied from 1 MHz to 170 MHz. The aforementioned studies, however, require sophisticated fabrication techniques such as electron beam lithography.

In the present study, the authors aimed to establish a process for fabricating a carbon-based MEMS. The authors fabricated cantilevers by using a conventional MEMS fabrication technology [8, 9] and HOPG, which does not require a high-temperature process or high-energy cutting.

2. Fabrication Process

2.1 Fabrication Method

Our aim was to fabricate a complex device consisting

*Corresponding author: Junji Sone, Ph.D., Professor, research fields: MEMS (micro-electromechanical systems), mechanical design and 3D printing. E-mail: sone@cs.t-kougei.ac.jp.

of micro- and nano-electromechanical systems using a typical MEMS fabrication process. The authors used the exfoliation method to prepare HOPG microsheets, as other chemical methods cannot produce 1 μm thick films for MEMS devices. The initial stage of the fabrication process is as follows: the HOPG microsheet was exfoliated almost 10 times using adhesive tape to produce a 3 μm thick HOPG sheet. A tantalum coating (40 nm) was applied by sputtering one side of the sheet. The HOPG sheet with its tantalum coat was attached to a Si plate by using a resist and a hot plate. In the second stage, the HOPG microsheet was polished, and its thickness was reduced to 0.5 μm on soft rubber by using wet sandpaper numbers 2,000, 3,000 and 6,000. The resulting surface roughness was almost 0.1 μm . Subsequently, a tantalum coating was applied by sputtering the side of the sheet to polish.

The cantilever pattern was formed by using a resist. The upper tantalum coat (outside pattern) was subjected to wet etching. The HOPG microsheet (outside pattern) and resist were removed by O_2 ashing. The tantalum film of the outside pattern and the cantilever underneath were removed by XeFe_2 dry etching [10], which is the appropriate dry-etching technique for SiO_2 and Si.

In our first trial, we directly used an exfoliated HOPG microsheet with a thickness of more than 2 μm and surface roughness of 0.5 μm . Such a thickness requires a long fabrication process, which leads to damage of the HOPG microsheet, because it takes 50 min for completion of O_2 ashing. Therefore, the cantilever

was non-functional.

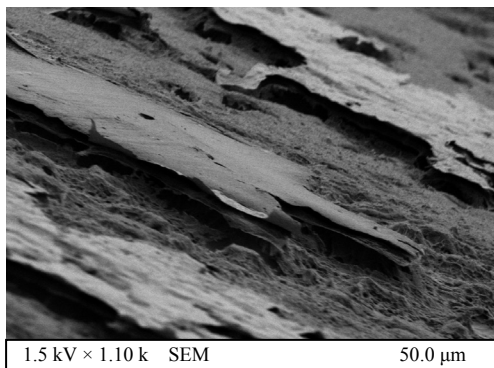
In our second trial, we polished and exfoliated the HOPG microsheet to allow the cantilever to function and the fabrication process for the doubly clamped beam. We used wet sandpaper numbers 2,000, 3,000, and 6,000 to reduce the thickness of the microsheet to around 500 nm. Fig. 1 shows a SEM image of the cantilever after O_2 ashing. A uniform HOPG microsheet was formed because of the polishing of the exfoliated HOPG microsheet.

3. Fabrication Results

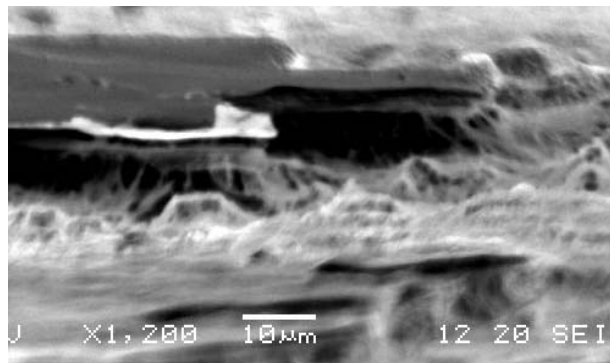
Fig. 1 shows the fabricated cantilever and the clearance between the HOPG microsheet and resist layers. In this case, the clearance was almost 40 nm. High-resolution observation was difficult because the electron beam damages carbon. Fig. 2 displays the results of the frequency measurement (Polytec MSA-500 micro system analyzer, vacuum conditions). We confirmed by Raman spectroscopy (Jusco NRS-3100) that the HOPG microsheet was on the surface of the cantilever (Fig. 3). Figs. 4-6 show an image of another fabricated cantilever, results of the frequency measurement and Raman spectra of the cantilever, respectively. We observed peaks for G and D bands in the Raman spectra.

Table 1 shows the theoretical and measured resonance frequencies of the cantilever. The first resonance frequency f is given by Eqs. (1) and (2):

$$f = \frac{1}{2\pi} \left(\frac{1.875}{L} \right)^2 \sqrt{\frac{EI}{\rho A}} \quad (1)$$



(a) Cantilever: C5



(b) Clearance of cantilever

Fig. 1 SEM image of over all of C5 cantilever and clearance.

Table 1 Theoretical and measurement resonance frequency of cantilevers: *b* is beam width, *L* is beam length and *t* is beam thickness, surface indicates surface roughness.

Name	<i>b</i> (μm)	<i>L</i> (μm)	<i>t</i> (μm)	Calc. (kHz)	Meas. (kHz)	Ratio	Surface
C5	7	32	0.5	2,050	720	0.351	Smooth
C11	15	20	0.5	5,024	1,243	0.247	Smooth
C13	6	44	0.5	1,080	497	0.460	Rough
C19	12	15	0.5	9,310	1,195	0.128	Rough

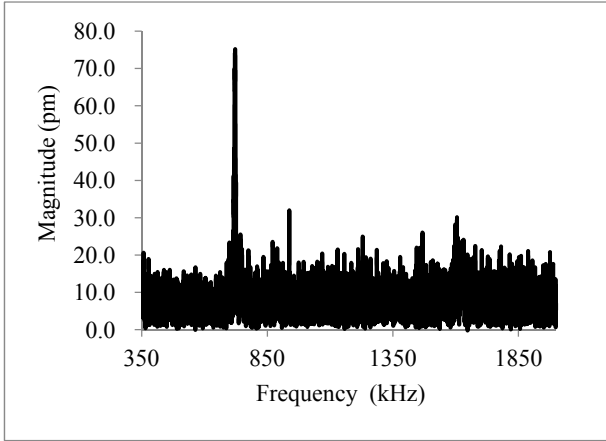


Fig. 2 Resonance frequency of cantilever: C5.

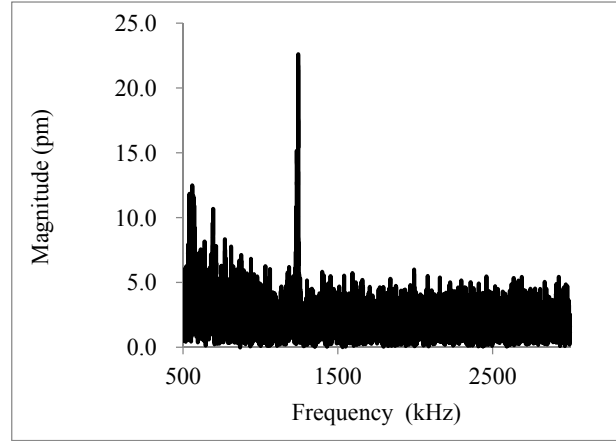


Fig. 5 Resonance frequency of cantilever: C11.

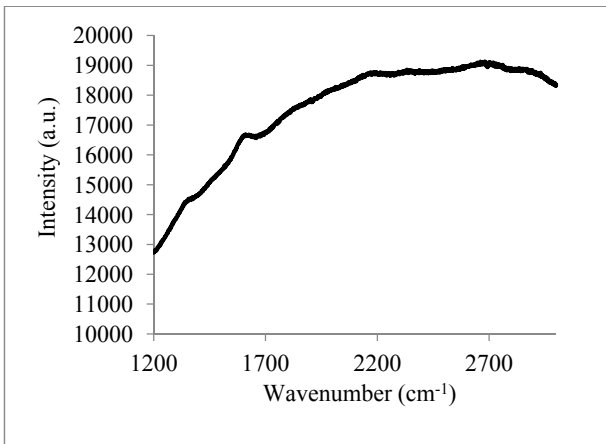


Fig. 3 Raman spectra of the cantilever: C5.

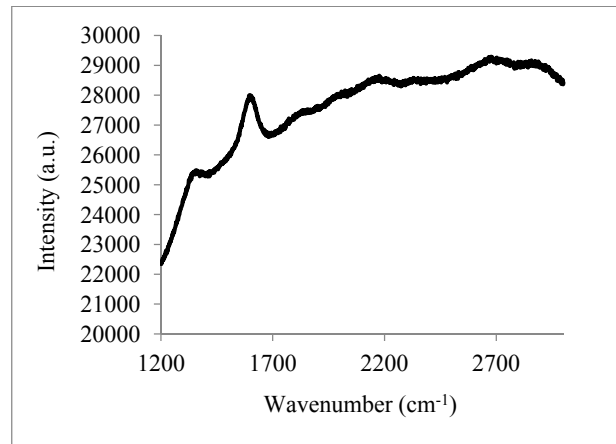


Fig. 6 Raman spectra of the cantilever : C11.

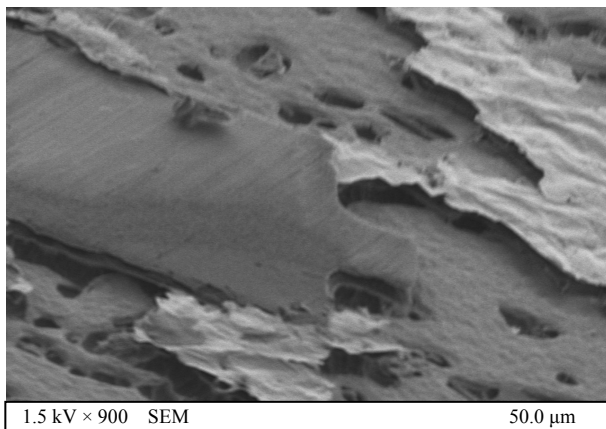


Fig. 4 SEM image of C11 cantilever.

$$I = \frac{bt^3}{12} \tag{2}$$

where, *L* is the beam length, *b* is the beam width, *t* is the beam thickness, and *A* is the cross-sectional area of the beam. ρ (2,226 kg/m³), *E* is Young’s modulus. We used an *E* value of 1,500 GPa (graphene) in the computations.

The ratio of the measured frequency to the computed resonance frequency is approximately 0.13-0.46. Figs. 1 and 4 show that, C5 had a thick region and a thickness that was more uniform than

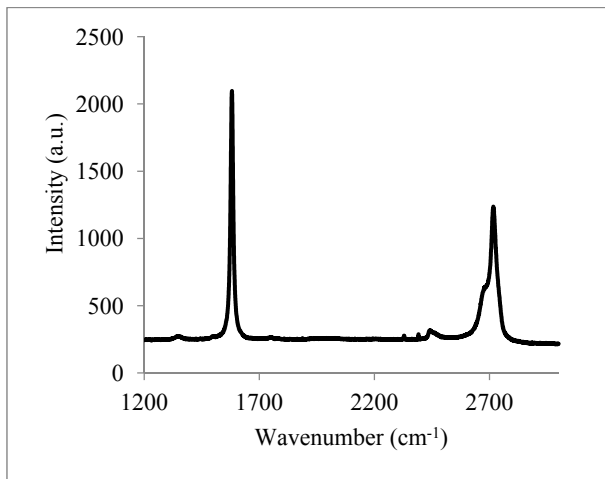
that of C11. Thus, the ratio of the measured frequency to the calculated resonance frequency of C5 was slightly higher than that of C11. The resonance frequency was probably affected by the nonuniform surface thickness and the numerous cracks in C5. As discussed later, we believe that reduction is the cause of the measured resonance frequency.

Fig. 7 shows the Raman spectra of the HOPG microsheet and of the tantalum film formed by sputtering. Spectra in Figs. 3 and 6 also suggest defects (D band, peak at around $1,400\text{ cm}^{-1}$) and the effect of tantalum. The property of the HOPG microsheet declined relative to the original value. One main effect was O_2 ashing, which is a plasma-based process. The tantalum film was removed by HF

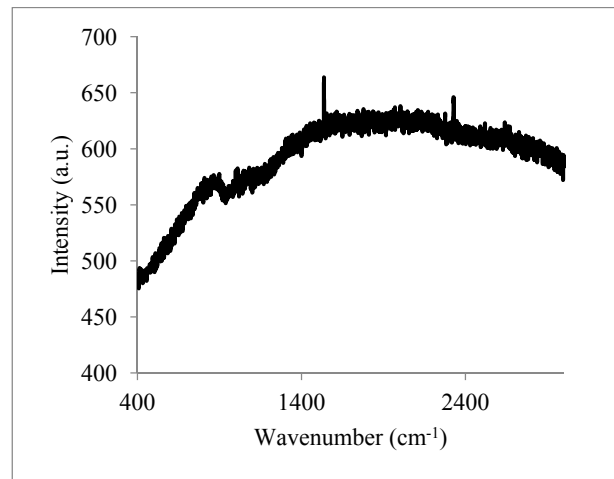
(hydrofluoric acid) etching. Because the strong adhesion of tantalum to carbon, it was difficult to completely remove tantalum from the surface of the cantilever.

We also fabricated a doubly clamped beam. Figs. 8-10, respectively shows SEM images and clearance, frequency data, and Raman spectra for DB501. High-resolution observation was difficult because the electron beam damages carbon. Fig. 8b shows the clearance between the HOPG microsheet and resist layers. Similar results for DB150 are shown in Figs. 11-13.

Table 2 lists the theoretical and measured resonance frequencies. The first resonance frequency of the doubly clamped beam is expressed by Eq. (3):

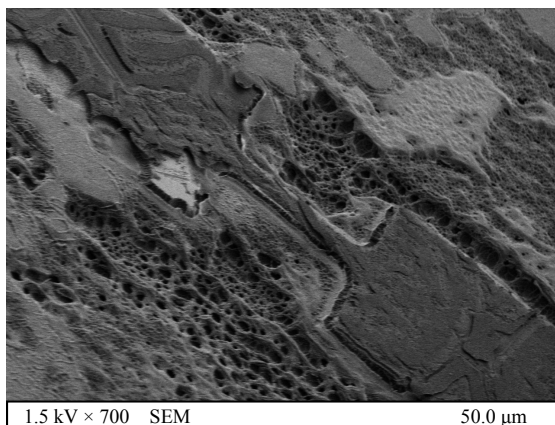


(a) HOPG film

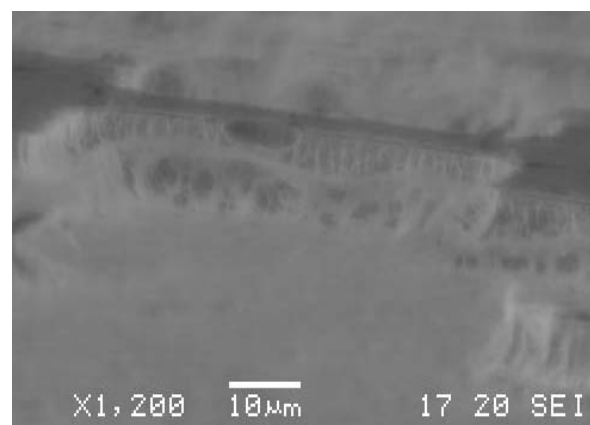


(b) Tantalum film

Fig. 7 Raman spectra of the HOPG film and tantalum film.



(a) Doubly clamped beam: DB501



(b) Clearance of doubly clamped beam

Fig. 8 SEM image of over all of DB501 doubly clamped beam and clearance.

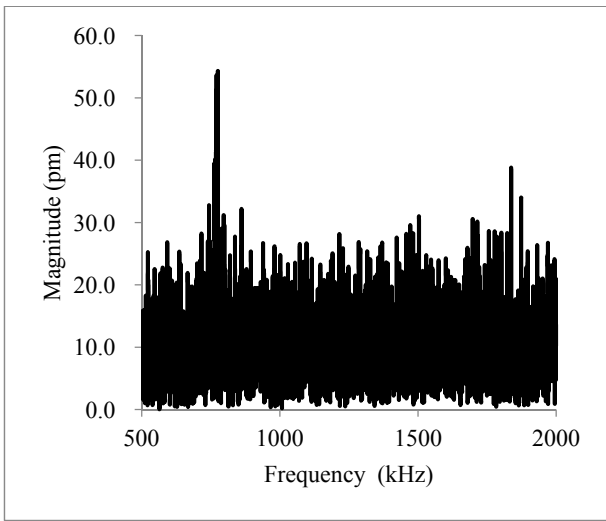


Fig. 9 Resonance frequency of doubly clamped beam: DB501.

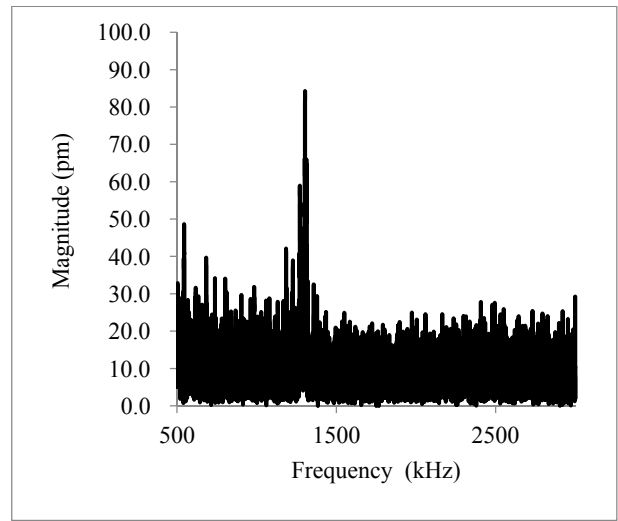


Fig. 12 Resonance frequency of doubly clamped beam: DB150.

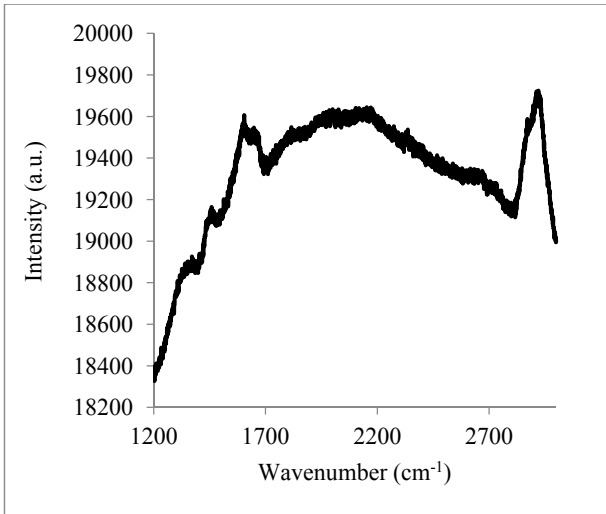


Fig. 10 Raman spectra of the doubly clamped beam: DB501.

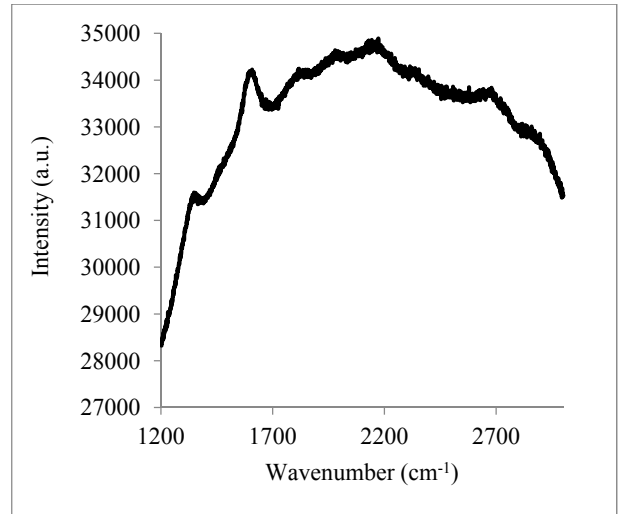


Fig. 13 Raman spectra of the doubly clamped beam: DB150.

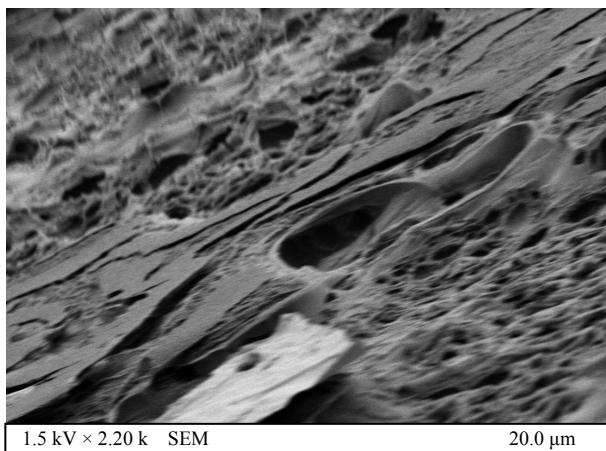


Fig. 11 SEM image of over all of DB150 doubly clamped beam.

$$f = \frac{1}{2\pi} \left(\frac{4.73}{L} \right)^2 \sqrt{\frac{EI}{\rho A}} \quad (3)$$

where, L is the beam length, b is the beam width, t is the beam thickness, and A is the cross-sectional area of the beam. $\rho = 2,226 \text{ kg/m}^3$. We used an E value of 1,500 GPa (graphene) for the theoretical calculation. The ratio of measured to theoretical resonance frequencies is 0.01-0.18. DB150 has deep cracks (Figs. 8 and 11), suggesting that the ratio for DB150 was smaller than that of DB501. The resonance frequency of DB150 was probably affected by the non-uniform surface thickness and its numerous cracks. As

Table 2 Theoretical and measurement resonance frequency of doubly clamped beam: b is beam width, L is beam length and t is beam thickness, surface indicates surface roughness.

Name	b (μm)	L (μm)	t (μm)	Calc. (kHz)	Meas. (kHz)	Ratio	Surface
DB501	10	56	0.5	4250	770	0.181	Rough
DB115	5	16	0.5	52,120	545	0.010	Rough
DB150	19	24	0.5	23,160	1,303	0.056	Rough
DB201	15	55	0.5	4,410	780	0.177	Rough
DB202	15	26	0.5	19,740	1,057	0.054	Rough
DB310	8	57	1.0	8,213	1,313	0.160	Rough

discussed later, we believe that reduction is the cause of the measured resonance frequency. Additionally, the effect of O_2 ashing and tantalum on the Raman spectra suggests the presence of defects (D band).

4. Discussion

The measured resonance frequencies of the cantilever were less than half of their theoretical counterparts. The authors attribute this lower resonance frequency to cracks, rough edges and thickness variations. Such cracks, which resulted from exfoliation, generated numerous regions of small curvature. In particular, the authors believe that the beam contained numerous cracks in its interior and on its surface, which reduced the beam's stiffness. Results of the experimental study [11], suggest that one crack reduces the resonance frequency of the cantilever by almost 5%; this value is dependent on the crack depth and location. Thus, if the beam has 30 cracks, the resonance frequency is nearly 0.2 times that of the original value. This value is dependent on the condition and number of the cracks. Thus, the ratio was consistent with our measurements of the resonance frequency. In addition, preparation of a HOPG microsheet with fewer cracks was of prime importance in our study. Defects suggested by the Raman spectra indicate the need to reconsider the patterning process, especially the O_2 ashing step. The Raman spectra are also affected by the strong adhesion of tantalum to carbon. The authors will thus reconsider the coating material and leave space for vibrations.

The authors also fabricated a doubly clamped beam

and found that its resonance frequencies were more than one-fifth of the theoretical values. The authors attribute the decrease in resonance frequency to cracks, rough edges, and thickness variations. The authors also believe that the cracks mainly reduced the stiffness of the beam; numerous cracks in the interior and on the surface of the cantilever reduced the resonance frequency. Adhesion of tantalum to carbon caused damage to the beam and affected the Raman spectra. Therefore, we need to develop a fabrication protocol that results in less damage and higher accuracy.

5. Conclusions

The authors developed a carbon-based MEMS device via a typical MEMS fabrication process. The authors used an exfoliated HOPG microsheet to maximize its performance. Thickness variations of the cantilever were minimized by polishing the HOPG microsheet.

The cantilever beams (C5, C11) that we constructed have an identical resonance frequency to that of silicon. The authors believe that the use of the HOPG microsheet is advantageous to the fabrication of thin MEMS devices with thicknesses less than 500 nm. Obtaining defect-free crystals is difficult; however, if the authors can reduce the number of defects in the HOPG microsheet, then the authors can build MEMS springs and devices that are more compact and exhibit better performance.

In future research, the authors will improve the quality of the HOPG microsheet. The authors will use the exfoliation method, although it is not suitable for

formation of film with less damage. The authors plan to improve the quality of the HOPG microsheet. This may be achieved through using CVD (chemical vapor deposition) [12, 13], however, it requires innovation that would enable generation of a 0.5 μm thick microsheet. Another possible method is conversion from a DLC (diamond like carbon) microsheet [14]. Furthermore, the authors will fabricate a mechanical spring and sensor to add useful functions to the MEMS device.

Acknowledgments

This work was supported by “Nanotechnology Platform” of the MEXT (Ministry of Education, Culture, Sports, Science and Technology), Japan, at the Center for Integrated Nanotechnology Support, Tohoku University. We want to thank Naoki Inomata, Kentaro Totsu, Shuji Tanaka, Masayoshi Esashi (Tohoku University) for support and discussion of research.

References

- [1] Iijima, S. Nanocarbon Materials: Synthesis and Structure Characterization. *2nd Workshop on Nanoscience: Carbon-Related Systems and Nanomaterials* **2012**, 3-7.
- [2] Cleland, A. N. *Foundations of Nanomechanics: From Solid-State Theory to Device Applications*; Springer-Verlag: New York, 2003; pp 349-405.
- [3] Schueller, J. A. O.; Brittain, T. S.; Whitesides, M. G. Fabrication of Glassy Carbon Microstructures by Soft Lithography. *Sensors and Actuators* **1999**, *A72*, 125-139.
- [4] Wang, C. A Novel Method for the Fabrication of High-Aspect Ratio C-MEMS Structures. *Journal of Microelectromechanical Systems* **2005**, *14*(2), 348-358.
- [5] Rose, F.; Debray, A.; Martin, P.; Fujita, H.; Kawakatsu, H. Suspended HOPG Nanosheets for HOPG Nanoresonator Engineering and New Carbon Nanostructure Synthesis. *Nanotechnology* **2006**, *17*, 5192-5200.
- [6] Chen, C.; Rosenblatt, S.; Bolotin, K. I.; Kalb, W.; Kim, P.; Kymissis, I.; et al. Performance of Monolayer Graphene Nanomechanical Resonators with Electrical Readout. *Nature Nanotechnology* **2009**, *4*, 861-867.
- [7] Bunch, J. S. Electromechanical Resonators, from Graphene Sheets. *Science* **2007**, *315*, 490-493.
- [8] Gad-el-Hak, M. *MEMS: Design and Fabrication*; CRC Press: 2005; pp 1-112.
- [9] Esashi, M. *Microsensors and Microactuators for Biomedical Applications, Nanofabrication and Biosystems*; Cambridge Univ. Press: 1996; pp 61-79.
- [10] Toda, R.; Minami, K.; Esashi, M. Thin Beam Bulk Micromachining Based on RIE and Xenon Difluoride Silicon Etching. *Sensors and Actuators* **1998**, *A66*, 268-272.
- [11] Morassi, A.; Vestroni, F. *Dynamic Methods for Damage Detection in Structures*; Springer: 2008; pp 83-193.
- [12] Ago, H.; Ogawa, Y.; Tsuji, M.; Mizuno, S.; Hibino, H. Catalytic Growth of Graphene: towards Large-Area Single-Crystalline Graphene. *J. Phys. Chem. Lett.* **2012**, *3*(16), 2228-2236.
- [13] An, H.; Lee, W.; Junga, J. Graphene Synthesis on Fe Foil Using Thermal CVD. *Current Applied Physics* **2011**, *11*(4), S81-S85.
- [14] Sone, J., Shigeta, N.; Yamada, K.; Uchida, T.; Yoshida, S.; Hayasaka, T.; et al. Annealing Transformation of Diamond-Like Carbon Using Ni Catalyst. *Jpn. J. Appl. Phys.* **2013**, *52*, 128005.